Climate Dynamics
https://doi.org/10.1007/s00382-021-05788-8

A dynamical pathway bridging African biomass burning and Asian summer monsoon

Dianbin Cao[1] · Tae-Won Park[2] · Yongjia Song[3] · Yuhang Wang[3] · Zhenyu You[3] · Yanluan Lin[1] · Yi Deng[3]

Received: 24 November 2020 / Accepted: 26 April 2021

Abstract
The Asian summer monsoon (ASM) affects more than one-third of the world's population due to its close connection with floods, droughts thus water resources in densely populated Asian countries. The effects of aerosols emitted in remote regions on the ASM, in contrast to local emissions, remain largely unclear. Here we demonstrate through a hierarchy of climate models that aerosol emissions from the central African wildfires could strengthen the circulation of the ASM (South Asian Monsoon in particular), increase precipitation over South Asia and reduce precipitation immediately north and south of it. The enhanced latent heating over South Asia provides a critical positive feedback to the initial strengthening of monsoon westerlies associated with wildfire-driven anomalous Rossby wave source. The atmospheric dynamical bridge discovered here effectively connects African biomass burning with hydroclimate variability over East Asia in boreal summer and offers a new source of monsoon predictability across a range of timescales.

Keywords Asian summer monsoon · African wildfires · Rossby wave source · Atmospheric dynamical bridge

1 Introduction

The Asian summer monsoon (ASM) (Fig. 1a) exhibits variability across a wide range of temporal scales (Lau et al. 2000) with atmospheric aerosols being one of the important factors contributing to such variability. Aerosols do so through directly absorbing and scattering solar radiation and indirectly modifying the microphysical and optical properties of clouds (Twomey 1977; Albrecht 1989; Ackerman et al. 2000; Rosenfeld et al. 2008). The associated changes of atmospheric heating structure result in a variety of ASM responses. For example, black carbon (BC) absorbs solar radiation and heats the atmosphere. Depending on the altitude of its presence, BC could strengthen or weaken atmospheric convection (Chung and Zhang 2004). Earlier observational and modeling studies revealed that this effect might contribute to the long-term trends of flooding (drought) in the southern (northern) China (Menon 2002; Jiang et al. 2013), and strengthen the South Asian monsoon circulation during the early-monsoon season due to the BC accumulation in the northern India near the Himalayas referred to as the "elevated heat pump" (EHP) (Lau et al. 2006, 2008; Lau and Kim 2006). Correspondingly, "solar dimming" (Stanhill and Cohen 2001; Liepert 2002) related to both absorbing and scattering aerosols may lead to the cooling of land surface, reduce the boreal summer land-sea thermal contrast, and ultimately inhibits the monsoon circulation over both East Asia (Qian et al. 2011; Song et al. 2014) and South Asia (Ramanathan et al. 2005; Chung and Ramanathan 2006; Bollasina et al. 2011).

Several modeling studies have argued that the collective opposing effects of EHP and solar dimming are responsible for an earlier onset of ASM, i.e., the intensified pre-monsoon rainfall and inhibited total precipitation during the monsoon season (Lau and Kim 2007; Meehl et al. 2008; Collier and Zhang 2009; Bollasina et al. 2013). While most earlier work focused on the impacts of local aerosols on atmospheric circulation, the effects of aerosols of remote origins were also highlighted in a few modeling studies (Cowan and Cai 2011; Ganguly et al. 2012). The key argument is

✉ Yi Deng
yi.deng@eas.gatech.edu

1 Ministry of Education Key Laboratory for Earth System Modeling, Department of Earth System Science, Tsinghua University, Beijing, China

2 Department of Earth Science Education, Chonnam National University, Gwangju, South Korea

3 School of Earth and Atmospheric Sciences, Georgia Institute of Technology, Atlanta, GA, USA

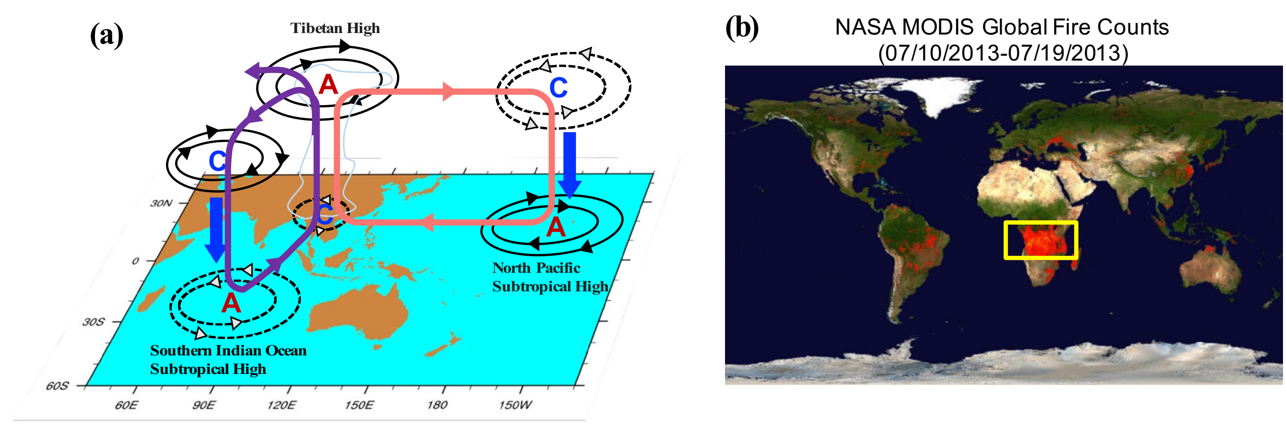

Fig. 1 **a** Schematic diagram of the ASM circulation in horizontal and vertical direction. **b** The spatial distribution of fire counts (red dots) between July 10th and 19th in 2013 based on the MODIS product. The fire counts in the central Africa (the yellow box) are much higher than those over other parts of the world

that remote aerosols can modify atmospheric diabatic heating and consequently excite large-scale atmospheric disturbances that propagate to downstream regions (Ming et al. 2010, 2011; Ming and Ramaswamy 2011). For example, it has been shown in an idealized model setting that the zonally asymmetric response to the uniform aerosol forcing is closely linked to the Rossby waves excited by anomalous atmospheric heating over the tropical Eastern Pacific (Ming et al. 2011). The relative roles of local versus remote aerosol forcing on the ASM still remain controversial. Specifically, non-local aerosols may contribute to the intensified rainfall over India favoring an earlier monsoon onset in June and increase rainfall over the northwestern India (Bollasina et al. 2014). A new modeling study looking at different aerosol species found that non-local sulfur dioxide aerosols account for about 75% of the simulated rainfall decease over India (Guo et al. 2016). The impacts of West Asian and Arabian dust particles on the ASM have also been noted (Vinoj et al. 2014; Solmon et al. 2015).

Biomass burning, mostly accounted for by wildfires, acts as a major source of aerosol emission across the globe. Figure 1b shows the global wildfire occurrences between July 10th and 19th in 2013 based on the NASA Moderate Resolution Imaging Spectroradiometer (MODIS) product. Most significant biomass burnings are found over South America and the central and southern Africa. By analyzing projected changes in temperature and precipitation, recent studies have shown that the potential of wildfire over some regions is increasing under climate change associated with greenhouse gas forcing and these include both South America and the southern Africa (Running 2006; Liu et al. 2010). There are also quite a number of studies exploring the impact of wildfires on gas and aerosol emissions (Spracklen et al. 2007, 2009; Lehsten et al. 2009; Jaffe and Wigder 2012), health (Finlay et al. 2012; Chen et al. 2017), radiative forcing (Ward et al. 2012; Jiang et al. 2016; Lu et al. 2018; Brown et al. 2018), global and regional climate change (Viereck 1973; Yoshikawa et al. 2002; Jacobson 2004; Tosca et al. 2013; Thornhill et al. 2018; Amiri-Farahani et al. 2020; Jiang et al. 2020) and local weather systems (Rosenfeld 1999; Andreae 2004; Grell et al. 2011), even though the dynamical processes bridging local and/or remote wildfire emissions and regional climate remain largely unclear.

Given the tremendous impact of the ASM on nearly half of the world's population and the major biomass burning occurring near Eurasia (e.g., central Africa wildfires), our study aims to answer the following two questions: Firstly, are there detectable effects of aerosol emissions from wildfires on the characteristics of the ASM including the circulation and precipitation? Secondly, if there are detectable effects, what dynamical processes are involved? Here we conduct a series of climate model experiments to identify the potential footprints of remote wildfire aerosols left in the ASM circulation and rainfall pattern and to understand the dynamical origins of these footprints. Our results indicate that the inclusion of forcing from wildfire aerosols in the model increases the strength of the ASM circulation and meridionally redistributes monsoonal rainfall over East Asia. A dynamical bridge is proposed to explain the connection between African wildfires and the ASM in boreal summer.

2 Methods

2.1 Model and experiment design

As an atmospheric component of the Community Earth System Model (CESM) version 1.2, the Community Atmosphere Model Version 5.0 (CAM5) was used as the main modeling tool to extract the footprints of wildfires on the

ASM. In the framework of CESM, CAM5 is coupled with the community land model version 4.5 (CLM4.5) (Oleson et al. 2010). CAM5 includes improved schemes of radiation, moisture turbulence (Bretherton and Park 2009), shallow and deep convection (Zhang and McFarlane 1995; Park and Bretherton 2009), and two-moment cloud macrophysics and microphysics (Morrison and Gettelman 2008; Gettelman et al. 2010). The 3-mode Modal Aerosol Model (MAM3) (Ghan et al. 2012) is also implemented in CAM5 to simulate the aerosol lifecycle. In MAM3, the aerosol mass and number mixing ratio are simulated in three lognormal modes: Aitken, accumulation, and coarse mode. BC and primary organic matter (POM) from wildfires and anthropogenic sources are emitted into the accumulation mode. It allows explicit treatment of aerosol–cloud interactions, better representations of the aerosol direct and indirect effects and thus reasonable capture of the aerosol signature in CAM5 (Liu et al. 2012). A comprehensive introduction of CAM5 includes more detailed descriptions (Neale et al. 2010).

In this study, we conducted two sets of AMIP-type ensemble experiments for the period 2001–2010 using the CAM5 at a horizontal resolution of $2.5° \times 1.9°$ with 26 hybrid sigma-pressure levels in the vertical. Each set includes 10 ensemble members. The two sets of ensembles were forced by the same boundary conditions including time-dependent monthly sea surface temperature and sea-ice concentration and used the same external radiative forcing. They only differ by the aerosol emissions: one set (NO-FIRE run) considers just the anthropogenic aerosol emissions based on the Precursors of Ozone and their Effects in the Troposphere (POET) emission data; the other set (FIRE run) further incorporates the natural wildfire aerosol emissions based on the Global Fire Emissions Database, Version 3 (GFEDv3) (Randerson et al. 2012) besides the anthropogenic aerosol emissions. The initial conditions of the 10 ensemble members were taken from 1-day model output at a 2-h interval (0 a.m., 2 a.m., …, 18 p.m.) from an existing CAM5 simulation. To generate vertical profiles of aerosol emissions, we conducted offline 1-D model simulations using fire plume height datasets obtained from the GFED and the fire emissions are distributed towards the top of a fire plume with a half-Gaussian shape giving maximum injection at the top (Freitas et al. 2010).

2.2 Idealized GCM

The idealized GCM was also used in the study to delineate and verify the response of the ASM circulation to the fire-induced large-scale diabatic cooling anomaly over the central Africa. This idealized GCM is a global, hydrostatic, primitive equation model based upon the spectral dynamical core of the NOAA GFDL Flexible Modeling System (FMS). All simulations were conducted at T85 horizontal resolution with 20 sigma levels in the vertical. Forced by Newtonian relaxation toward a prescribed, zonally symmetric temperature profile characteristic of the boreal summer (JJA), the model was first integrated for 300 days to achieve a near-steady-state solution to realistic topography. At day 300, the Newtonian relaxation was turned off and replaced by the JJA mean, 3-dimensional diabatic heating rates derived from the NO-FIRE CAM5 simulations. The model flow is quasi-steady over the period day 304–328. The model was then restarted from Day 304 and a large-scale cooling anomaly with a Gaussian shape centered about 400 hPa corresponding to a maximum cooling of -0.3 K/day was added to the diabatic heating field. The new model integration with the added "thermal perturbation" is steady in the period day 5–36. The zonal wind, streamfunction and velocity potential averaged over day 5–29 from the "thermal perturbation" experiment were then subtracted by the same fields averaged over day 304–328 from the previous run to get the response of the model ASM to the prescribed cooling anomaly over the central Africa.

3 Results

3.1 Wildfire-induced aerosol changes in the model experiments

Figure 2 shows the simulated 10-year mean difference of aerosol optical depth (AOD) (Fig. 2a) and aerosol mass concentration (AMC) (Fig. 2b–f) between the FIRE and NO-FIRE cases. The most significant aerosol anomaly in terms of both AOD and AMC is found over the central Africa, especially between 5° N and 15° N. This elevated aerosol concentration is closely tied to wildfires occurring in this region and in regions south of the equator (Fig. 1b) with the fire emission from the Southern Hemisphere being transported northward by low-level southwesterlies of the west African monsoon and by southerlies/southeasterlies over the central Africa. The wildfire-related aerosols over the central Africa are mostly primary organic matters (POM) (Fig. 2c). Sulfate, BC, and secondary organic matters (SOM) also have nontrivial contributions (Fig. 2d–f). These results suggest that the CAM5 model has decent skills in simulating the wildfire-induced changes in AOD and AMC with their significant increases occurring over regions of elevated fire emissions.

3.2 Wildfire-induced changes in the circulation strength of the Asian summer monsoon

The widely accepted Webster–Yang monsoon index (WYI) (Webster and Yang 1992), defined as the difference of the zonal wind between 850 and 200 mb averaged over South

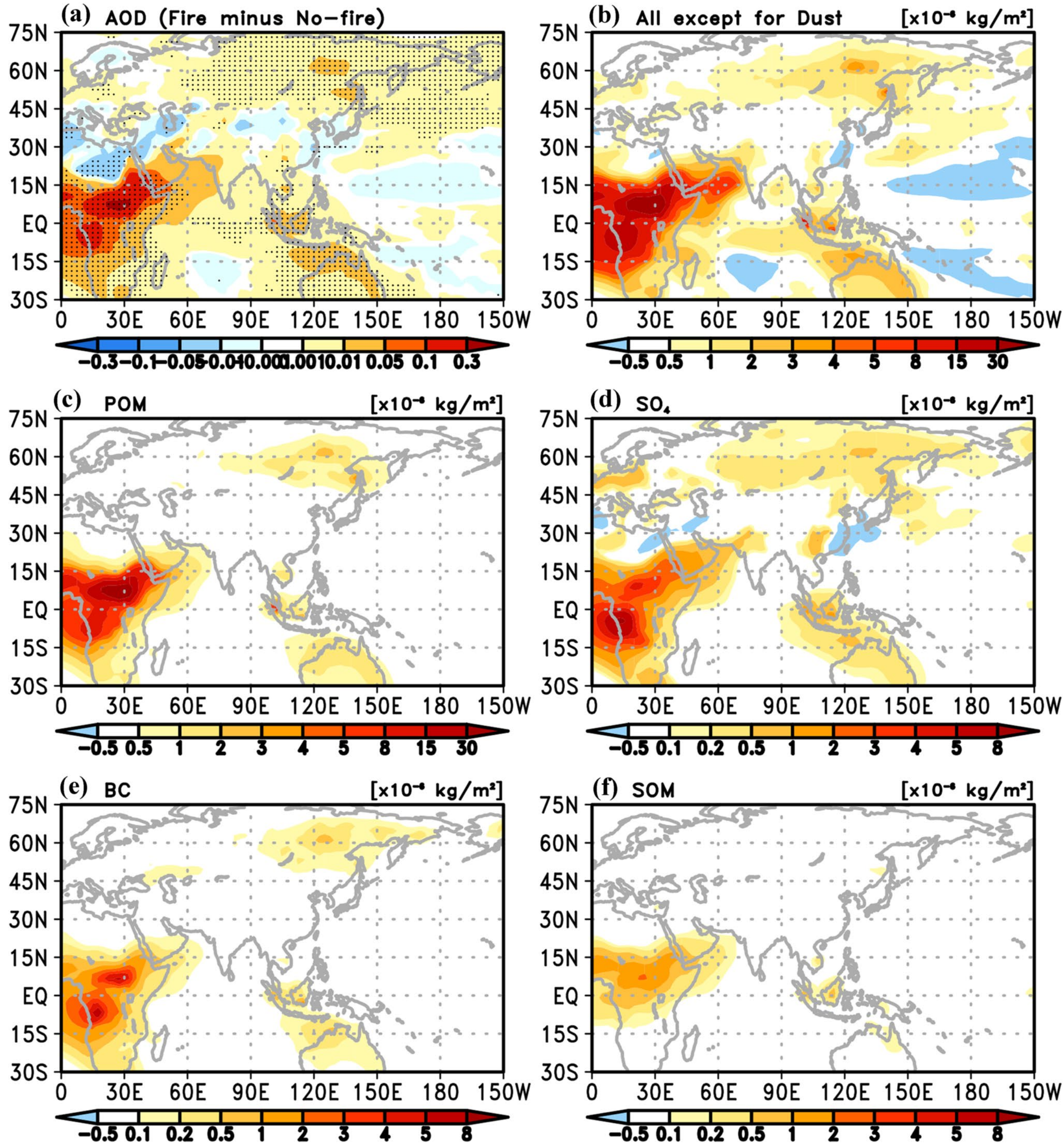

Fig. 2 Fire-induced changes in the AOD and the AMC. 10-year mean differences between FIRE and NO-FIRE ensembles of **a** AOD (areas significant at the 0.01 level are denoted by dots), as well as AMC of **b** all particles excluding the dust aerosols, **c** primary organic matters (POM), **d** sulfate (SO4), **e** black carbon (BC), and **f** secondary organic matters (SOM)

Asia (5° N–20° N and 40° E–110° E) is adopted as a measure of the intensity of the monsoon circulation and computed for each boreal summer (June–July–August, JJA) using in the CAM5 outputs. Figure 3 shows the climatological evolution of the daily WYI in JJA for both the FIRE and NO-FIRE run. The FIRE run is clearly characterized by a stronger monsoon circulation compared to the NO-FIRE run, especially during the peak season of the ASM (Fig. 3a). In terms of the JJA-mean WYI, 7 out of 10 ensemble members indicate the presence of a stronger monsoon in FIRE runs

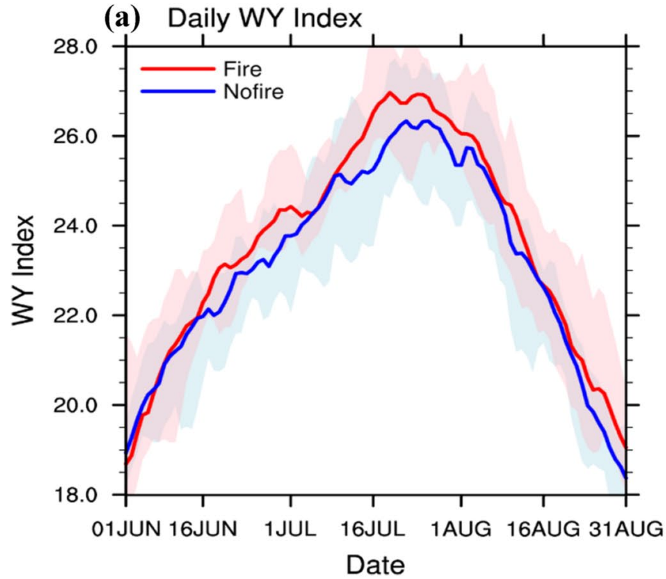

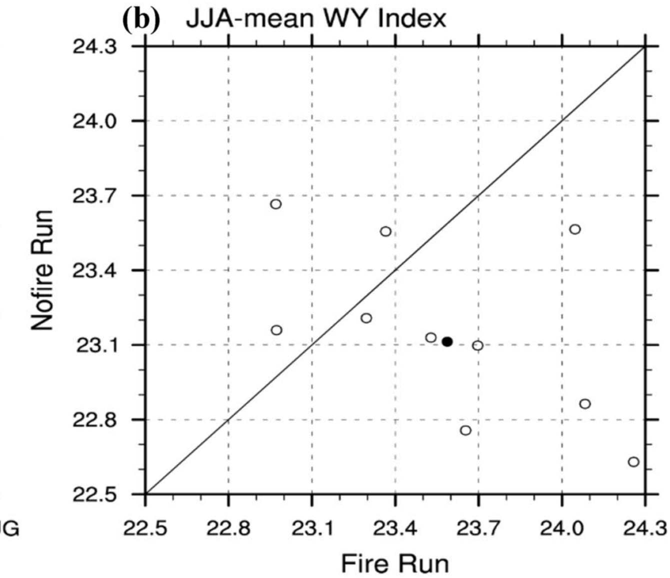

Fig. 3 Fire-induced changes in the strength of the ASM circulation. **a** The time evolution of the ensemble mean of the WYI in JJA. The red line is for FIRE runs and the blue line is for NO-FIRE runs. Red and blue shading indicates the corresponding spread among ensemble members. **b** The JJA-mean WYI of the 10 ensemble members from FIRE and NO-FIRE runs (open circles). The black solid point represents the ensemble mean. The black solid line indicates the reference line where y = x

(Fig. 3b). The ensemble-averaged WYI in JJA is about 2.5% higher (significant at the 0.01 level) in the FIRE run than that in the NO-FIRE run with the largest increase among all ensemble members being around 8.5%.

3.3 Dynamics behind the wildfire-induced strengthening of the monsoon circulation

The increased intensity of the monsoon circulation associated with wildfires is also evident in the 850 hPa wind field, a key component in the construct of the WYI. Figure 4a, c show the JJA-mean 850 hPa zonal and total wind in the NO-FIRE run, respectively. The model reasonably reproduces the classic ASM circulation including westerlies over South Asia associated with the lower level cyclonic circulation, and the cross-equatorial monsoonal flow. Including aerosol emissions by wildfires lead to an acceleration of the monsoon westerlies (Fig. 4b) and an overall strengthening of the monsoon flow (Fig. 4d) over South Asia.

To understand how the westerly acceleration is achieved in the CAM5 simulation, we diagnose the Rossby wave source (RWS, Sardeshmukh and Hoskins 1988) in both the FIRE and NO-FIRE runs.

$$S = -\eta D - v_\chi \cdot \nabla \eta = -\nabla \cdot (v_\chi \eta) \qquad (1)$$

In Eq. (1) above, S stands for the RWS; η is the absolute vorticity; D is the divergence and v_χ represents the velocity of the divergent flow that can be obtained from the velocity potential χ. S is the sum of two parts: $-\eta D$ representing the generation of vorticity by divergence (stretching term), and $-v_\chi \dot{\nabla}\eta$ representing the generation of vorticity through the advection of absolute vorticity by the divergent flow.

Figure 4e, f shows, respectively, the fire-induced changes of the JJA-mean velocity potential and stream function at 850 hPa. Wildfire emissions drive a negative velocity potential anomaly over the north-central Africa and a positive anomaly over the Arabian Sea (colored shading in Fig. 4e) projecting positively into the climatological velocity potential distribution in the NO-FIRE run (contours in Fig. 4e). Corresponding to such velocity potential anomalies are anomalous divergent westerlies centered about 15° N (black arrow in Fig. 4e). As shown in Fig. 4f, the anomalous divergent westerlies effectively produce a positive anomalous (FIRE minus NO-FIRE) RWS over Arabian Sea through the stretching term in Eq. (1), more specifically, through a combination of the positive climatological (NO-FIRE) absolute vorticity and the anomalous (FIRE minus NO-FIRE) convergence. The anomalous divergent westerlies also lead to a positive anomalous RWS downstream of the climatological 850 hPa vorticity maxima corresponding to the monsoon cyclone (contours in Fig. 4f) via the divergent flow advection term in Eq. (1) (i.e., positive advection of the climatological vorticity by the anomalous divergent flow). In a similar way, the climatological divergent flow works with the anomalous vorticity to generate anomalous positive RWS extending from the Arabian Sea to India. Compared to these two processes, the combination of the anomalous divergent flow

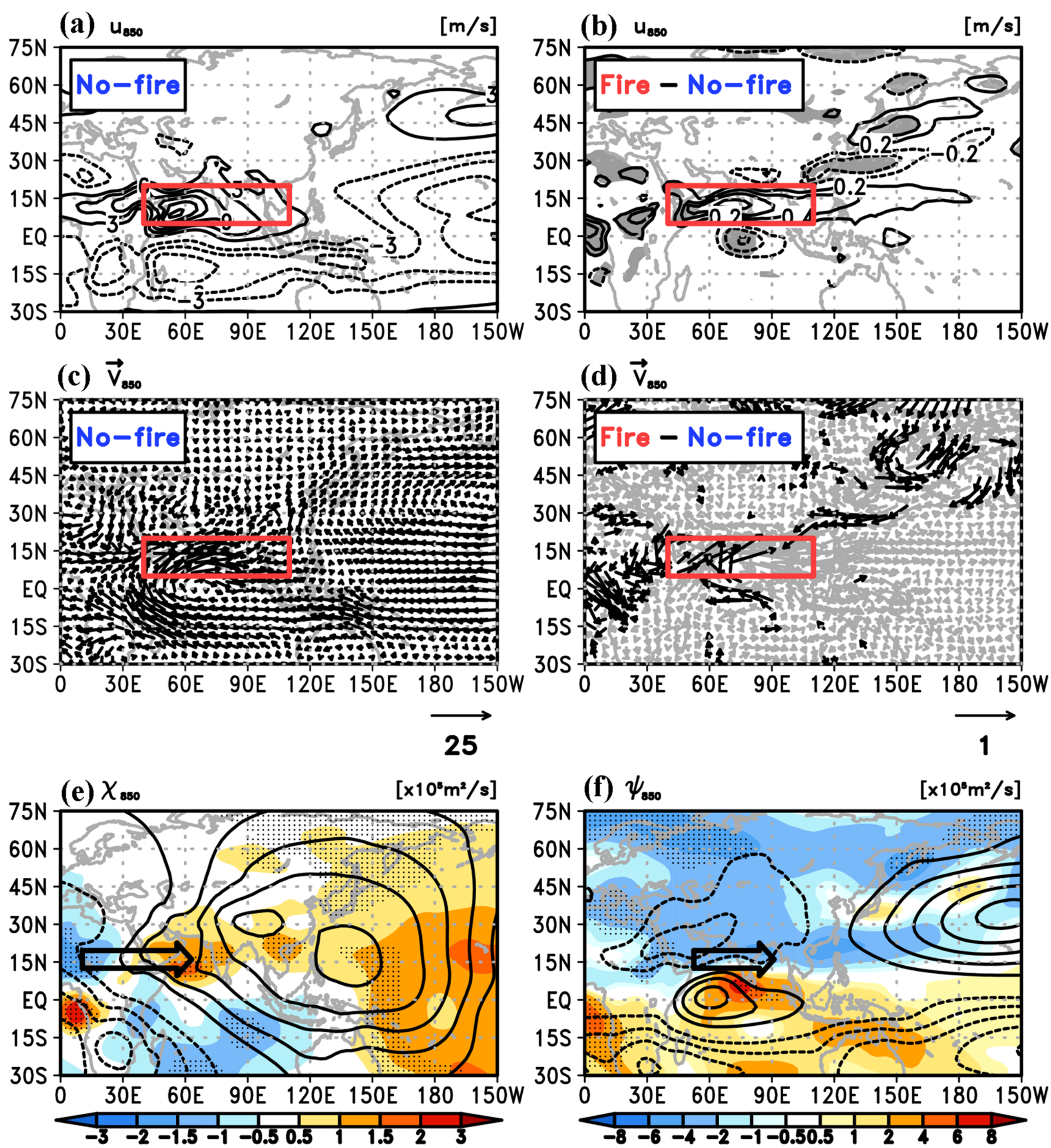

Fig. 4 Fire-induced changes in the ASM circulation. **a** Zonal wind at 850 hPa under NO-FIRE runs. **b** Same as **a** except for the difference between FIRE and NO-FIRE runs. **c** Total wind at 850 hPa under NO-FIRE runs. **d** Same as **c** except for the difference between FIRE and NO-FIRE runs. **e** Velocity potential at 850 hPa of NO-FIRE runs (black contours) and the difference between FIRE and NO-FIRE runs (color shading). **f** Same as **e** except for streamfunction at 850 hPa. Areas significant at the 0.01 level are shaded in **b**, indicated by black arrows in **d**, and denoted by dots in **e** and **f**. The red boxes (5° N–20° N and 40° E–110° E) mark the area used in the calculation of the WYI. The black arrows in **e** and **f** represent the anomalous divergent and rotational westerlies, respectively

and anomalous vorticity also provides a positive yet much weaker contribution to the overall anomalous positive RWS over South Asia. The positive RWS leads to enhanced rotational westerlies over the Arabian Sea, India, and the Bay of Bengal, adding to the initial divergent westerly anomalies, and ultimately drive the westerly acceleration and the strengthening of the monsoon flow seen in Fig. 4b, d.

3.4 Wildfire-induced changes in monsoonal rainfall and large-scale diabatic heating

The change in the monsoon circulation is also reflected by changes in the distribution of the monsoonal rainfall. As shown in Fig. 5a, the fire-induced rainfall change is characterized by below-normal rainfall over the Yangtze River valley in China extending to the southern Japan, over the equatorial Indian ocean and the Maritime Continent, and by above-normal rainfall across South Asia extending to the tropical western Pacific. This tri-pole structure in rainfall change is consistent with the fire-induced changes in the JJA mean lower tropospheric moisture convergence shown in Fig. 5b. Over the central Africa where the largest wildfire emission is found (Fig. 2a), rainfall is suppressed (Fig. 5a). Through reduced latent heating, this rainfall reduction is largely responsible for the negative diabatic heating anomaly that peaks between 300 and 500mb over this region (black curve, Fig. 5d). The positive (negative) diabatic heating anomaly found over South Asia (the tropical Indian Ocean and Maritime Continent) also suggests the key role played by the latent heating change (blue and red curve in Fig. 5d). Given the majority of the wildfire-related emissions being scattering aerosols such as POM, SO4 and SOM (Fig. 2c, d, f), the diabatic cooling anomaly found over the central Africa is likely contributed by both aerosols' direct effect

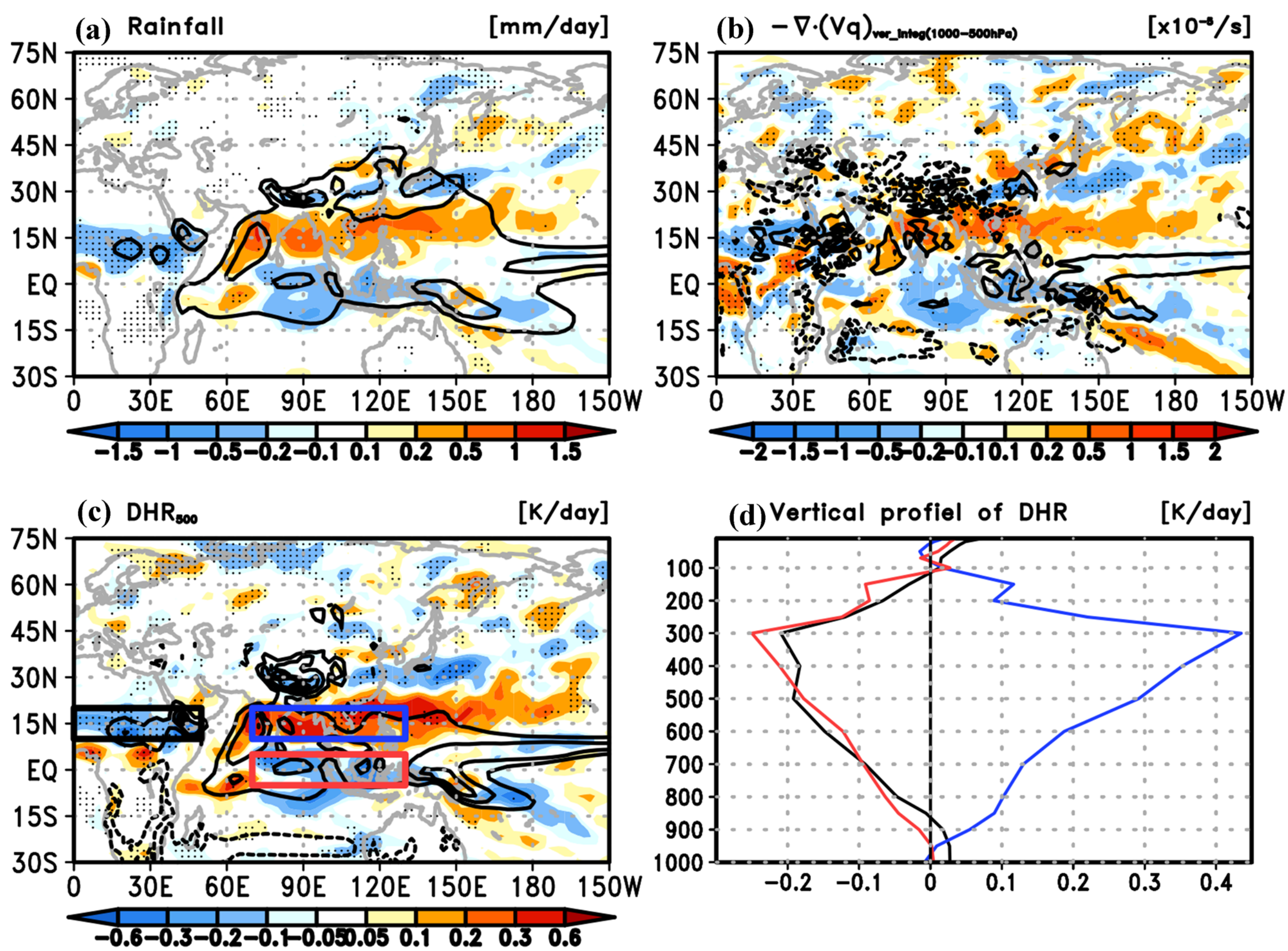

Fig. 5 Fire-induced changes in the monsoonal rainfall, moisture and diabatic heating. JJA-mean of **a** rainfall, **b** convergence of moisture flux vertically integrated from 1000 to 500 hPa, and **c** diabatic heating rate (DHR) at 500 hPa. The black contours are for NO-FIRE runs and the color shading is for the difference between FIRE and NO-FIRE runs. Areas significant at the 0.01 level are denoted by dots. The black, blue, and red curves in **d** are the corresponding vertical profiles of DHR (the difference between FIRE and NO-FIRE runs) averaged over the black, blue, and red box in **c**, respectively

and indirect effect (e.g., via enhanced cloud albedo and rainfall suppression). The atmospheric heating associated with BC is relatively weak due to its small concentration compared to other scattering aerosols (Fig. 2e), and is completely masked by the reduced latent heating (anomalous cooling effect) discussed above.

3.5 Thermal perturbation experiments and a dynamical pathway bridging African wildfire and ASM

To connect fire-induced changes in large-scale heating and the dynamical processes leading to the acceleration of the monsoon westerlies, we carried out additional "thermal perturbation" experiments using an idealized dry global circulation model (GCM). A summer basic state was first established in the dry GCM with the topography and diabatic heating derived from NO-FIRE runs as the model forcing. A thermal perturbation was then added to the diabatic heating field of the model forcing corresponding to a patch of cooling anomaly over the central Africa as shown in Fig. 6a (for details, please see "Methods"). Figure 6b–d show the changes of the lower-tropospheric circulation induced by this prescribed large-scale cooling anomaly. Westerly acceleration similar to the fire-induced one in CAM5 can be identified at the 850 hPa level in the dry GCM (Fig. 6b). The anomalous velocity potential (Fig. 6c) and stream function (Fig. 6d) over the tropical Indian Ocean and Asia forced by the cooling anomaly also qualitatively resembles the fire-induced response of the monsoon circulation shown in Fig. 4. Therefore, the introduction of a diabatic cooling anomaly over the central Africa effectively reproduces the key feature of fire-induced changes in the monsoon circulation.

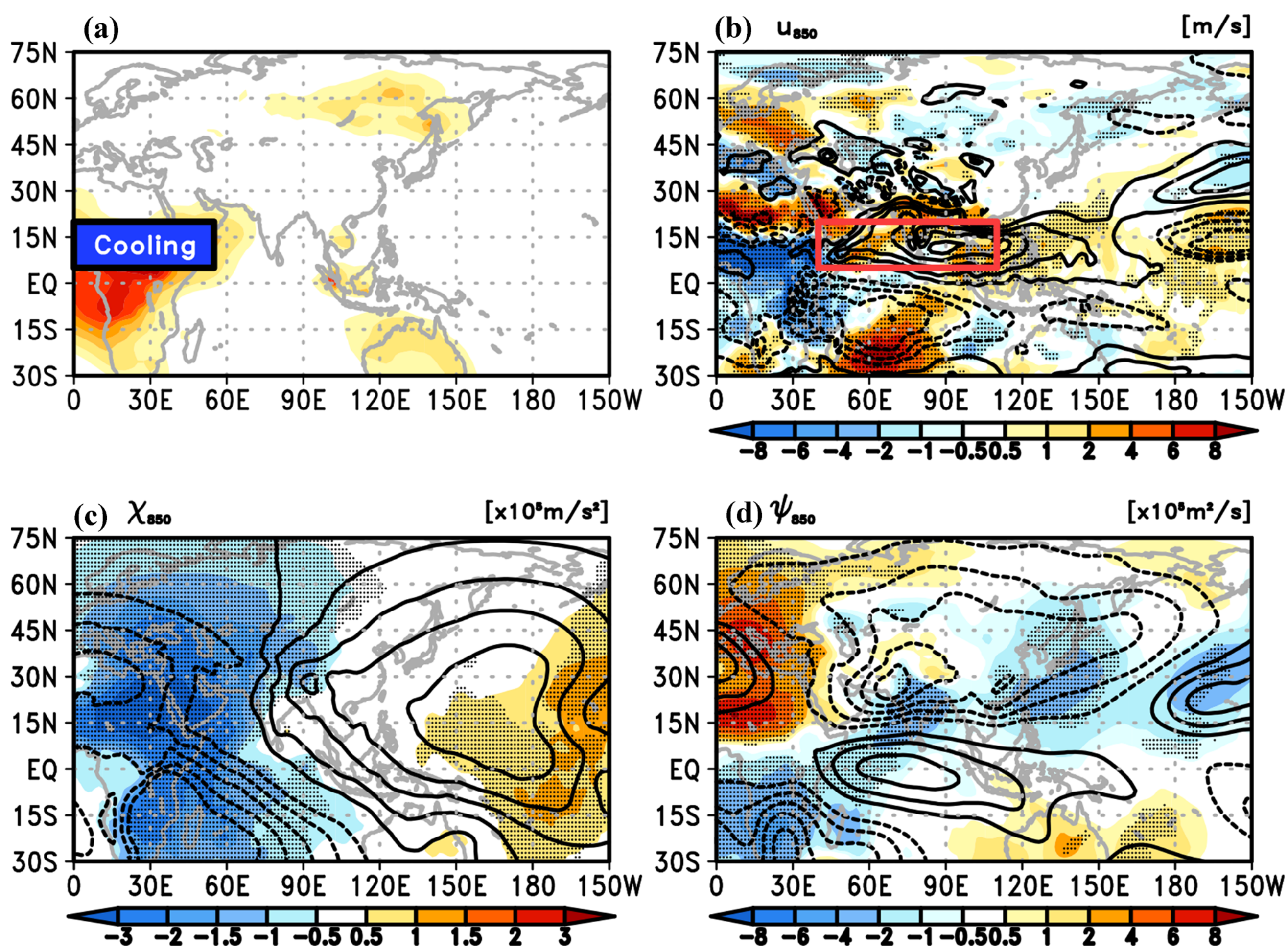

Fig. 6 The response of the atmospheric circulation to the prescribed thermal perturbation over the central Africa in an idealized dry GCM. **a** Location of the thermal perturbation corresponding to a diabatic cooling anomaly over the central Africa (blue box). **b** Zonal wind at 850 hPa for the basic state (black contours) and the change resulted from the thermal perturbation (color shading). The red box is the same as that in Fig. 4. **c** Same as **b** except for velocity potential at 850 hPa. **d** Same as **b** except for stream function at 850 hPa. Areas significant at the 0.01 level are denoted by dots

Given both the CAM5 and the dry GCM results, here we propose a dynamical pathway that bridges African wildfire and ASM (Fig. 7): aerosol emissions from the African wildfire generate anomalous cooling over the central Africa through both aerosol's direct scattering effect and indirect effect that increases cloud albedo and reduce latent heating due to rainfall suppression; the anomalous cooling drives anomalous large-scale descent over the central Africa and leads to anomalous divergent westerlies and subsequently anomalous rotational westerlies across the Arabian Sea, India and the Bay of Bengal through the creation of anomalous Rossby wave source; the increased low-level moisture convergence over South Asia as a result of the westerly acceleration generates above-normal rainfall in the region with rainfall suppressed over regions to its immediate south and north due to the extra-consumption of moisture over South Asia; then the positive latent heating anomaly resulted from the above-normal rainfall over South Asia further enhances the lower tropospheric heating contrast between Africa and South Asia and leads to even stronger divergent westerlies between the two regions ultimately providing a positive feedback to the changes of the monsoon circulation and rainfall initiated by the fire-induced cooling over the central Africa.

4 Discussion

The variations in the ASM rainfall accounts for a significant portion of the hydroclimate fluctuations over East Asia and South Asia (Gadgil 2003; Webster et al. 2012). It modulates flood and drought conditions in this region leaving tremendous impacts on mankind and natural systems (Bhalme and Mooley 1980; Sanyal and Lu 2004). Atmospheric aerosols' effects on monsoons are also being increasingly recognized (Twomey 1977; Albrecht 1989; Rosenfeld et al. 2008; Menon 2002; Lau and Kim 2006; Ramanathan et al. 2005; Bollasina et al. 2011; Meehl et al. 2008; Ganguly et al. 2012; Ming et al. 2011; Andreae 2004). Wildfires as

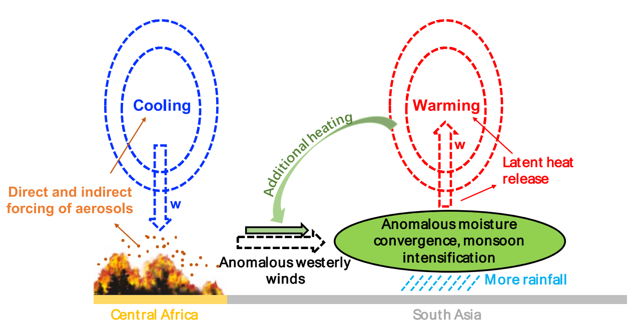

Fig. 7 Schematic diagram of a dynamical pathway bridging African wildfires and the ASM

an important source of aerosols have been occurring more frequently in the past few decades (Running 2006; Liu et al. 2010) and affecting many elements vital for human survival like biodiversity, vegetation productivity, air quality, and water quality (Flannigan et al. 1998; Yoshikawa et al. 2002; Westerling et al. 2003; Meixner and Wohlgemuth 2004). For example, the vegetation-rich Amazon forest is a region of growing concern with observational evidence that aerosols produced by Amazon wildfires are influencing local weather and climate (Andreae 2004; Cochrane and Barber 2009). Elevated wildfire activities might also affect ecosystems and local climate including Western US (Westerling et al. 2003; Spracklen et al. 2007, 2009), Alaska (Viereck 1973; Yoshikawa et al. 2002), Africa (Lehsten et al. 2009), and etc.

Our modeling and diagnostic study for the first time demonstrated the existence of a plausible dynamical pathway bridging aerosol emissions of African biomass burning and the ASM suggesting that African wildfires can remotely modulate the ASM, especially the South Asian monsoon (SAM) circulation strength and rainfall distribution. This finding fills a gap in our understanding of the remote and external factors influencing the ASM variability and further broadens our view of the multiple roles played by wildfires in the Earth's climate system. This newly discovered dynamical connection between Africa and Asia in boreal summer also offers a potentially new source of predictability of the ASM across sub-seasonal to decadal timescales assuming skillful predictions and projections of African wildfire activity can be made. We would also like to point out that all conclusions drawn here are based on simulations conducted with a hierarchy of atmospheric models. Additional experiments with comprehensive Earth System Models (ESMs) are needed to quantify the relative importance of the wildfire effects on the ASM in comparison to other known factors such as air-sea interaction and to investigate the likely collective effects of multiple factors on the variability and trends of the ASM.

Finally, identifying the actual footprints of wildfires in the ASM from real observations is a much more challenging task since multiple external (e.g., greenhouse gases, anthropogenic aerosols, volcano eruptions) and internal (e.g., oceanic modes of variability such as the ENSO, PDO and IOD) factors affect the ASM, and wildfire effects are unlikely to be prominent enough to decide the overall trend and variability of the ASM. This means that our findings in this modeling analysis are not contradicting the observed increasing trend in the African wildfire activity and the decreasing Asian summer monsoon intensity in the recent decades. A preliminary analysis of satellite and reanalysis products has been carried out to verify the existence of the proposed dynamical pathway connecting African wildfires with the ASM, specifically to connect African biomass burning emissions with local diabatic heating anomalies. By contrasting years of elevated African fire activity with those of reduced fire activity, we found that more aerosol emissions from wildfires increased upward shortwave flux at the TOA through enhanced (cloud) albedo (direct and first indirect effect), increased cloud fraction, suppressed rainfall (second indirect effect), and increased outgoing longwave radiation (OLR) via increased cloud top temperature. These change of the radiative flux at the TOA implies a net radiative cooling of the atmosphere, which, combined with the reduced latent heating due to rainfall suppression, leads to a net diabatic cooling over the central Africa, consistent with findings from our modeling experiments. The years of elevated African fire activity are also characterized by slightly increased low-level westerlies over the Arabian Sea, suggesting a strengthened SAM circulation. Given the large uncertainty involved in isolating fire effects from direct observations (e.g., interferences from multiple external/internal factors) and the imperfect representation of fire and aerosol effects in models, these preliminary results of observational data analyses lend further support to the conclusions drawn here although further investigations in this direction are warranted.

Acknowledgements The authors thank two anonymous reviewers for their constructive review comments. Deng was in part supported by the National Science Foundation Climate and Large-Scale Dynamics (CLD) program through Grants AGS-1354402 and AGS-1445956 and by the National Oceanic and Atmospheric Administration through award NA16NWS4680013. D. Cao was supported by the Tsinghua University Initiative Scientific Research program through grant 2019Z07L01001 and by the Tsinghua University Visiting Scholar program under award number 2018113. Y. Wang, Y. Song, and T.-W. Park were supported by the National Science Foundation (NSF) through Grant 1243220. T.-W. Park was also supported by the National Research Foundation of the Korean government with the Grant number NRF-2020R1A4A3079510.

Data availability The global fire emissions database (GFED) is available at https://daac.ornl.gov/get_data/, and output data from the model runs are archived at Georgia Tech local servers and are publically available upon request.

Code availability All codes used to perform the analyses in this study are available on request from the corresponding author.

Declarations

Conflict of interest The authors declare no competing financial interests.

References

Ackerman AS, Toon OB, Stevens DE et al (2000) Reduction of tropical cloudiness by soot. Science 288:7. https://doi.org/10.1126/science.288.5468.1042

Albrecht BA (1989) Aerosols, cloud microphysics, and fractional cloudiness. Sci Wash 245:1227. https://doi.org/10.1126/science.245.4923.1227

Amiri-Farahani A, Allen RJ, Li K et al (2020) A La Niña-like climate response to South African biomass burning aerosol in CESM simulations. J Geophys Res Atmos 125:6. https://doi.org/10.1029/2019JD031832

Andreae MO (2004) Smoking rain clouds over the Amazon. Science 303:1337–1342. https://doi.org/10.1126/science.1092779

Bhalme HN, Mooley DA (1980) Large-scale droughts/floods and monsoon circulation. Mon Weather Rev 108:1197–1211. https://doi.org/10.1175/1520-0493(1980)108%3c1197:LSDAMC%3e2.0.CO;2

Bollasina MA, Ming Y, Ramaswamy V (2011) Anthropogenic aerosols and the weakening of the South Asian summer monsoon. Science 334:502–505. https://doi.org/10.1126/science.1204994

Bollasina MA, Ming Y, Ramaswamy V (2013) Earlier onset of the Indian monsoon in the late twentieth century: the role of anthropogenic aerosols. Geophys Res Lett 40:3715–3720. https://doi.org/10.1002/grl.50719

Bollasina MA, Ming Y, Ramaswamy V et al (2014) Contribution of local and remote anthropogenic aerosols to the twentieth century weakening of the South Asian Monsoon. Geophys Res Lett 41:680–687. https://doi.org/10.1002/2013GL058183

Bretherton CS, Park S (2009) A new moist turbulence parameterization in the Community Atmosphere Model. J Clim 22:3422–3448. https://doi.org/10.1175/2008JCLI2556.1

Brown H, Liu X, Feng Y et al (2018) Radiative effect and climate impacts of brown carbon with the Community Atmosphere Model (CAM5). Atmos Chem Phys 18:17745–17768. https://doi.org/10.5194/acp-18-17745-2018

Chen J, Li C, Ristovski Z et al (2017) A review of biomass burning: emissions and impacts on air quality, health and climate in China. Sci Total Environ 579:1000–1034. https://doi.org/10.1016/j.scitotenv.2016.11.025

Chung CE, Ramanathan V (2006) Weakening of North Indian SST gradients and the monsoon rainfall in India and the Sahel. J Clim 19:2036–2045. https://doi.org/10.1175/JCLI3820.1

Chung CE, Zhang GJ (2004) Impact of absorbing aerosol on precipitation: dynamic aspects in association with convective available potential energy and convective parameterization closure and dependence on aerosol heating profile. J Geophys Res Atmospheres 109:D22. https://doi.org/10.1029/2004JD004726

Cochrane MA, Barber CP (2009) Climate change, human land use and future fires in the Amazon. Glob Change Biol 15:601–612. https://doi.org/10.1111/j.1365-2486.2008.01786.x

Collier JC, Zhang GJ (2009) Aerosol direct forcing of the summer Indian monsoon as simulated by the NCAR CAM3. Clim Dyn 32:313–332. https://doi.org/10.1007/s00382-008-0464-9

Cowan T, Cai W (2011) The impact of Asian and non-Asian anthropogenic aerosols on 20th century Asian summer monsoon. Geophys Res Lett 38:11. https://doi.org/10.1029/2011GL047268

Finlay SE, Moffat A, Gazzard R et al (2012) Health impacts of wildfires. PLoS Curr 4. https://doi.org/10.1371/4f959951cce2c

Flannigan MD, Bergeron Y, Engelmark O, Wotton BM (1998) Future wildfire in circumboreal forests in relation to global warming. J Veg Sci 9:469–476. https://doi.org/10.2307/3237261

Freitas SR, Longo KM, Trentmann J, Latham D (2010) Technical note: sensitivity of 1-D smoke plume rise models to the inclusion of environmental wind drag. Atmos Chem Phys 10:2. https://doi.org/10.5194/acpd-9-14713-2009

Gadgil S (2003) The Indian monsoon and its variability. Annu Rev Earth Planet Sci 31:429–467. https://doi.org/10.1146/annurev.earth.31.100901.141251

Ganguly D, Rasch PJ, Wang H, Yoon J-H (2012) Climate response of the South Asian monsoon system to anthropogenic aerosols. J Geophys Res Atmos 117:D13. https://doi.org/10.1029/2012JD017508

Gettelman A, Liu X, Ghan SJ et al (2010) Global simulations of ice nucleation and ice supersaturation with an improved cloud scheme in the Community Atmosphere Model. J Geophys Res 115:D18. https://doi.org/10.1029/2009JD013797

Ghan SJ, Liu X, Easter RC et al (2012) Toward a minimal representation of aerosols in climate models: comparative decomposition of aerosol direct, semidirect, and indirect radiative forcing. J Clim 25:6461–6476. https://doi.org/10.1175/JCLI-D-11-00650.1

Grell G, Freitas SR, Stuefer M, Fast J (2011) Inclusion of biomass burning in WRF-Chem: impact of wildfires on weather forecasts. Atmos Chem Phys 11:5289–5303. https://doi.org/10.5194/acp-11-5289-2011

Guo L, Turner AG, Highwood EJ (2016) Local and remote impacts of aerosol species on Indian summer monsoon rainfall in a GCM. J Clim 29:6937–6955. https://doi.org/10.1175/JCLI-D-15-0728.1

Jacobson MZ (2004) The short-term cooling but long-term global warming due to biomass burning. J Clim 17:2909–2926. https://doi.org/10.1175/1520-0442(2004)017<2909:TSCBLG>2.0.CO;2

Jaffe DA, Wigder NL (2012) Ozone production from wildfires: a critical review. Atmos Environ 51:1–10. https://doi.org/10.1016/j.atmosenv.2011.11.063

Jiang Y, Liu X, Yang X-Q, Wang M (2013) A numerical study of the effect of different aerosol types on East Asian summer clouds and precipitation. Atmos Environ 70:51–63. https://doi.org/10.1016/j.atmosenv.2012.12.039

Jiang Y, Lu Z, Liu X et al (2016) Impacts of global open-fire aerosols on direct radiative, cloud and surface-albedo effects simulated with CAM5. Atmos Chem Phys 16:14805–14824. https://doi.org/10.5194/acp-16-14805-2016

Jiang Y, Yang X-Q, Liu X et al (2020) Impacts of wildfire aerosols on global energy budget and climate: the role of climate feedbacks. J Clim 33:3351–3366. https://doi.org/10.1175/JCLI-D-19-0572.1

Lau K-M, Kim K-M (2006) Observational relationships between aerosol and Asian monsoon rainfall, and circulation. Geophys Res Lett 33:21. https://doi.org/10.1029/2006GL027546

Lau WKM, Kim K-M (2007) 3 Does aerosol weaken or strengthen the Asian monsoon? Developments in earth surface processes. Elsevier, Amsterdam, pp 13–22

Lau K-M, Kim K-M, Yang S (2000) Dynamical and boundary forcing characteristics of regional components of the Asian summer monsoon. J Clim 13:2461–2482. https://doi.org/10.1175/1520-0442(2000)013%3c2461:DABFCO%3e2.0.CO;2

Lau KM, Kim MK, Kim KM (2006) Asian summer monsoon anomalies induced by aerosol direct forcing: the role of the Tibetan Plateau. Clim Dyn 26:855–864. https://doi.org/10.1007/s00382-006-0114-z

Lau K-M, Ramanathan V, Wu G-X et al (2008) The joint aerosol–monsoon experiment: a new challenge for monsoon climate research. Bull Am Meteorol Soc 89:369–384. https://doi.org/10.1175/BAMS-89-3-369

Lehsten V, Tansey K, Balzter H et al (2009) Estimating carbon emissions from African wildfires. Biogeosciences 6:349–360. https://doi.org/10.5194/bgd-5-3091-2008

Liepert BG (2002) Observed reductions of surface solar radiation at sites in the United States and worldwide from 1961 to 1990. Geophys Res Lett 29:611–614. https://doi.org/10.1029/2002GL014910

Liu Y, Stanturf J, Goodrick S (2010) Trends in global wildfire potential in a changing climate. For Ecol Manag 259:685–697. https://doi.org/10.1016/j.foreco.2009.09.002

Liu X, Easter RC, Ghan SJ et al (2012) Toward a minimal representation of aerosols in climate models: description and evaluation in the Community Atmosphere Model CAM5. Geosci Model Dev 5:709–739. https://doi.org/10.5194/gmd-5-709-2012

Lu Z, Liu X, Zhang Z et al (2018) Biomass smoke from southern Africa can significantly enhance the brightness of stratocumulus over the southeastern Atlantic Ocean. Proc Natl Acad Sci 115:2924–2929. https://doi.org/10.1073/pnas.1713703115

Meehl GA, Arblaster JM, Collins WD (2008) Effects of black carbon aerosols on the Indian monsoon. J Clim 21:2869–2882. https://doi.org/10.1175/2007JCLI1777.1

Meixner T, Wohlgemuth P (2004) Wildfire impacts on water quality. J Wildland Fire 13:27–35

Menon S (2002) Climate effects of black carbon aerosols in China and India. Science 297:2250–2253. https://doi.org/10.1126/science.1075159

Ming Y, Ramaswamy V (2011) A model investigation of aerosol-induced changes in tropical circulation. J Clim 24:5125–5133. https://doi.org/10.1175/2011JCLI4108.1

Ming Y, Ramaswamy V, Persad G (2010) Two opposing effects of absorbing aerosols on global-mean precipitation. Geophys Res Lett 37:13. https://doi.org/10.1029/2010GL042895

Ming Y, Ramaswamy V, Chen G (2011) A model investigation of aerosol-induced changes in boreal winter extratropical circulation. J Clim 24:6077–6091. https://doi.org/10.1175/2011JCLI4111.1

Morrison H, Gettelman A (2008) A new two-moment bulk stratiform cloud microphysics scheme in the Community Atmosphere Model, version 3 (CAM3). Part I: description and numerical tests. J Clim 21:3642–3659. https://doi.org/10.1175/2008JCLI2105.1

Neale RB, Gettelman A, Park S et al (2010) Description of the NCAR community atmosphere model (CAM 5.0). NCAR, Boulder. NCAR/TN-486+STR. http://www.cesm.ucar.edu/models/cesm1.0/cam/docs/description/

Oleson KW, Bonan GB, Feddema JJ et al (2010) Technical description of an urban parameterization for the Community Land Model (CLMU). NCAR, Boulder. https://doi.org/10.5065/D6K35RM9

Park S, Bretherton CS (2009) The university of Washington shallow convection and moist turbulence schemes and their impact on climate simulations with the Community Atmosphere Model. J Clim 22:3449–3469. https://doi.org/10.1175/2008JCLI2557.1

Qian Y, Leung LR, Ghan SJ, Giorgi F (2011) Regional climate effects of aerosols over China: modeling and observation. Tellus B Chem Phys Meteorol 55:914–934. https://doi.org/10.3402/tellusb.v55i4.16379

Ramanathan V, Chung C, Kim D et al (2005) Atmospheric brown clouds: Impacts on South Asian climate and hydrological cycle. Proc Natl Acad Sci 102:5326–5333. https://doi.org/10.1073/pnas.0500656102

Randerson JT, Chen Y, van der Werf GR et al (2012) Global burned area and biomass burning emissions from small fires. J Geophys Res Biogeosci 117:G4. https://doi.org/10.1029/2012JG002128

Rosenfeld D (1999) TRMM observed first direct evidence of smoke from forest fires inhibiting rainfall. Geophys Res Lett 26:3105–3108. https://doi.org/10.1029/1999GL006066

Rosenfeld D, Lohmann U, Raga GB et al (2008) Flood or drought: How do aerosols affect precipitation? Science 321:1309–1313. https://doi.org/10.1126/science.1160606

Running SW (2006) Is global warming causing more, larger wildfires? Science 313:927–928. https://doi.org/10.1126/science.1130370

Sanyal J, Lu XX (2004) Application of remote sensing in flood management with special reference to monsoon Asia: a review. Nat Hazards 33:283–301. https://doi.org/10.1023/B:NHAZ.0000037035.65105.95

Sardeshmukh PD, Hoskins BJ (1988) The generation of global rotational flow by steady idealized tropical divergence. J Atmos Sci 45:1228–1251. https://doi.org/10.1175/1520-0469(1988)045%3c1228:TGOGRF%3e2.0.CO;2

Solmon F, Nair VS, Mallet M (2015) Increasing Arabian dust activity and the Indian summer monsoon. Atmos Chem Phys 15:8051–8064. https://doi.org/10.5194/acp-15-8051-2015

Song F, Zhou T, Qian Y (2014) Responses of East Asian summer monsoon to natural and anthropogenic forcings in the 17 latest CMIP5 models. Geophys Res Lett 41:596–603. https://doi.org/10.1002/2013GL058705

Spracklen DV, Logan JA, Mickley LJ et al (2007) Wildfires drive interannual variability of organic carbon aerosol in the western U.S. in summer. Geophys Res Lett 34:16. https://doi.org/10.1029/2007GL030037

Spracklen DV, Mickley LJ, Logan JA et al (2009) Impacts of climate change from 2000 to 2050 on wildfire activity and carbonaceous aerosol concentrations in the western United States. J Geophys Res 114:D20. https://doi.org/10.1029/2008JD010966

Stanhill G, Cohen S (2001) Global dimming: a review of the evidence for a widespread and significant reduction in global radiation with discussion of its probable causes and possible agricultural consequences. Agric for Meteorol 107:255–278. https://doi.org/10.1016/S0168-1923(00)00241-0

Thornhill GD, Ryder CL, Highwood EJ et al (2018) The effect of South American biomass burning aerosol emissions on the regional climate. Atmos Chem Phys 18:5321–5342. https://doi.org/10.5194/acp-18-5321-2018

Tosca MG, Randerson JT, Zender CS (2013) Global impact of smoke aerosols from landscape fires on climate and the Hadley circulation. Atmos Chem Phys 13:5227–5241. https://doi.org/10.5194/acp-13-5227-2013

Twomey S (1977) The influence of pollution on the shortwave albedo of clouds. J Atmos Sci 34:1149–1152. https://doi.org/10.1175/1520-0469(1977)034%3c1149:TIOPOT%3e2.0.CO;2

Viereck LA (1973) Wildfire in the Taiga of Alaska. Quat Res 3:465–495. https://doi.org/10.1016/0033-5894(73)90009-4

Vinoj V, Rasch PJ, Wang H et al (2014) Short-term modulation of Indian summer monsoon rainfall by West Asian dust. Nat Geosci 7:308–313. https://doi.org/10.1038/ngeo2107

Ward DS, Kloster S, Mahowald NM et al (2012) The changing radiative forcing of fires: global model estimates for past, present and future. Atmos Chem Phys 12:10857–10886. https://doi.org/10.5194/acp-12-10857-2012

Webster PJ, Yang S (1992) Monsoon and Enso: selectively interactive systems. Q J R Meteorol Soc 118:877–926. https://doi.org/10.1002/qj.49711850705

Webster PJ, Magaña VO, Palmer TN et al (2012) Monsoons: processes, predictability, and the prospects for prediction. J Geophys Res Oceans. https://doi.org/10.1029/97JC02719@10.1002/(ISSN)2169-9291.TOGA1

Westerling AL, Gershunov A, Brown TJ et al (2003) Climate and wildfire in the western United States. Bull Am Meteorol Soc 84:595–604. https://doi.org/10.1175/BAMS-84-5-595

Yoshikawa K, Bolton WR, Romanovsky VE et al (2002) Impacts of wildfire on the permafrost in the boreal forests of Interior Alaska. J Geophys Res Atmos 107:D1. https://doi.org/10.1029/2001JD000438

Zhang GJ, McFarlane NA (1995) Sensitivity of climate simulations to the parameterization of cumulus convection in the Canadian climate centre general circulation model. Atmos Ocean 33:407–446. https://doi.org/10.1080/07055900.1995.9649539